

Stress concentration and buckling behaviour of shear loaded composite panels with reinforced cutouts

*S.J. Guo**

School of Engineering, Cranfield University, Bedfordshire, MK43 0AL, UK

Abstract

Numerical and experimental studies have been conducted to investigate the effect of reinforcements around cutouts on the stress concentration and buckling behaviour of a carbon/epoxy composite panel under in-plane shear load. Four different types of cutout reinforcements made of a range of materials were evaluated. In the analysis, finite element method and an analytical method based on the laminate theory were employed to perform parametric studies on the various reinforcement designs. Four test panels were then manufactured and tested to validate the analysis results. Good agreement was found between the analytical and test results. Based on the validated analytical models, the best cutout reinforcement was determined.

Keywords: Cutout reinforcement; buckling; stress concentrations; finite element analysis.

Introduction

It is well known that laminated composite materials are increasingly used in aircraft structures. Apart from having high specific stiffness and strength values, composites also offer great potential for tailoring structural design for weight saving and desirable mechanical behaviour against applied loads. This paper addresses reinforcement methods for cutouts in shear-loaded composite panels, which may be applicable to the design of aircraft shear panels, such as wing ribs and spar webs. Currently there are two major concerns with this application. Firstly, laminated composites have been regarded as inefficient to carry shear loads; therefore aluminium alloys are still preferred for fabricating the ribs of current transport aircraft wings. Secondly, cutouts in these structures are inevitable in order to provide lightening holes, passages for cables and pipes, and accessibility for assembly and maintenance inspections. These cutouts will result in high stress concentrations and reduced critical buckling loads in these panels. As the primary aircraft structures, such as the wing spars and cover panels, are increasingly made of carbon fibre composites, the demands for using composite ribs have also driven many researchers to investigate the capability of composite panels with cutouts under various forms of loadings.

Research in the buckling and postbuckling behaviour of laminated composite panels with cutouts has been carried out primarily for uniaxial compression load. In 1995-6, Nemesh published two comprehensive reviews of the research activities in this field [1-2]. According to the review Martin's work published in 1972 [3] appears to be among the first studies of the buckling and postbuckling behaviour of square composite plates with cutouts under uniaxial compression-loaded. In 1978, Knauss, Starnes and Henneke [4] published an experimental investigation of the buckling and failure characteristics of compression-loaded carbon/epoxy plates with a central circular cutout. Later on, Marshall et al [5, 6] investigated the stability of compression-loaded orthotropic plates with holes by analytical and experimental approaches. Investigation was also made into the effect of cutout sizes

* Corresponding author. Tel. +44 (0)1234 754628
Email: s.guo@cranfield.ac.uk (S. Guo)

and plate aspect ratio [7] and curvature effect [8] on the buckling response of composite plates with cutouts.

There have also been considerable research efforts devoted to shear-loaded panels with cutouts [e.g. 3, 9-14]. However research in the cutout reinforcement is very limited. In 1995, Eiblmeier and Loughlan [15] published their work on numerical analysis of buckling behaviour of a shear loaded square carbon/epoxy composite panel with a cutout that was reinforced by a 30 mm wide composite rings. It was noted that the reinforcement rings bonded on both sides of the cutout resulted in the maximum achievable critical buckling load. In another numerical study of stress concentration and stability of shear loaded plates with cutouts Pandey et al adopted the idea of flanged cutouts for composite panels [16]. The performance of the reinforced composite panel was numerically simulated and compared with an aluminium counterpart of the same cutout size and weight. The authors found that the composite plates showed significant dividends in reducing stress concentration and increasing buckling loads, and therefore composite ribs with flanged cutouts could provide weight savings and better load-carrying capabilities. However, this is only a numerical study. In reality it is difficult to fabricate flanged cutout reinforcement using composite materials especially the carbon/epoxy laminates.

In fact, the aforementioned reinforcement methods for cutouts in composite panels are mostly adapted from the metallic structures, for which flanged cutout reinforcement is indeed a simpler and low cost method for fabricating lightening or access holes. For example, elliptical flanged holes are typically used for crawl holes in lightly or moderately loaded rib webs in the wing and empennage applications. The strength of panels containing these holes can be determined by using empirical design curves or datasheets. For primarily loaded metallic structures, the standard circular or elliptical holes are reinforced by either a 45° flange around the edges of the cutouts or a 'donut' ring doubler bonded to the cutout perimeter. These kinds of local reinforcement are an effective way to reduce the weight penalty and the stress concentration around cutouts as well as to increase the critical buckling loads. Therefore, in this work these reinforcement methods, which have been proved to be effective for metallic structures and had some success with composite panels under compression load, were applied to shear loaded composite panels with cutouts. The aim was to perform a systematic study by both numerical modelling and experimental testing on the effectiveness of various reinforcement types and sizes.

The objective of this paper is to present the results of a study of shear-loaded carbon/epoxy composite square panels with cutouts that are reinforced in order to reduce the stress concentration and enhance the stability. The scope of this study includes numerical modelling by FEA and experimental tests. The panels contain circular cutouts of three sizes strengthened by different types of reinforcement. An orthotropic laminate with stacking sequence of $(+45/-45)_{ns}$ has been selected as example, which gives the highest shear buckling load [10]. Parametrical study has been conducted based on the numerical and experimental results. Conclusions are drawn on the selection of reinforcement ring material and size.

2. Theoretical and numerical methods

2.1 Theoretical approach

Theoretical methods do not exist for the exact solution of stresses around a cutout of a laminated plate. A method based on the theory developed by Greszczuk [17] provides an analytical solution to the elastic stress distribution around the perimeter of a circular hole in a thin, single layer, homogeneous orthotropic plate under a combination of in-plane loadings. Application of this method to a laminated composite plate leads to an approximate result for a number of reasons. Firstly laminated composite is not strictly

homogeneous. Secondly interlaminar stresses and load shedding near the ends of fibres at the cutout edge cannot be modelled by this method. Thirdly the method is only valid for an infinitely large laminate containing a central hole; hence the hole size effect on the calculated stress concentration has been ignored. When this method is applied to a laminated composite, the laminate is treated effectively as a single ply and stress analysis is performed by conducting coordinate transformation and replacing the lamina properties by the equivalent properties of the laminate. Therefore only a single average value of tangential stress at the hole edge at any angular position can be calculated analytically. The loading condition can be a combination of in-plane bi-axial direct and shear loads. In theory, this method is only valid under the following conditions: (1) laminates with certain layups for which there is no coupling between the in-plane direct and shear stiffness; (2) strain distribution is constant through the thickness; (3) cutout diameter is five times greater than the laminate thickness; (4) the distance between the cutout edge and the plate boundary is at least 1.5 times of the cutout diameter for sufficient accuracy. Despite of these limitations, this method provides a useful analytical tool for estimating the through-thickness average values of stress and strain at the cutout edge.

Details of the method and equations for stress analysis are available in the ESDU datasheets [18-19]. Based on this theory a computer code was developed for industrial applications [18], which has been employed in this paper for making comparisons with the FE results. It should be noted that this method is limited to un-reinforced circular cutouts and certain layup sequences, i.e. unidirectional or symmetric, balanced, and specially orthotropic laminates.

2.2. Finite Element Analysis

Finite element method has been employed to analyse reinforced cutouts and various laminate stacking sequences. In this study the commercial FE code MSC PATRAN /NASTRAN was employed as the numerical tool. In all numerical and experimental cases, constant shear stress was applied at the panel's loading edges, i.e. all the tests were "load-controlled".

Before modelling the composite panels, a validation test was performed with an isotropic plate made of aluminium alloy 7075 in order to find a suitable element type and meshing density. The material properties are listed in Table 1. The ESDU datasheet 75034 [20] provides a convenient and valid stress solution around a circular hole for such a plate under shear loading. The square panel had the dimension of 320 x 320 mm with a central circular cutout of diameter 44 mm. The panel was simply supported and subjected to a shear load of 20 N/mm along its edges. The plate was modelled by 4-noded shell elements with increasingly refined mesh density towards the edge of the hole. When the mesh density was increased from 300 to 2400 and finally to 4700, the error in the calculated maximum stress was reduced from 9.3% to 2% and finally to 1% using [20] as the benchmark. Therefore in the following analysis, mesh density of 2400 was selected for efficient computation and sufficient accuracy.

3. Un-reinforced cutout

3.1 Example

A square panel of 320 x 320 mm and 2 mm thick with a central circular cutout was taken as example (Fig. 1). The panel was made of 16-ply carbon/epoxy pre-preg with the stacking sequence of $(\pm 45)_{4S}$ and material properties listed in Table 1. Three cutout sizes were modelled: $d = 44, 64$ and 160 mm.

3.2 Effect of cutout size on maximum stress

Firstly the laminate strains were determined by FE analysis and then the stresses in each layer in the two material principle directions were calculated. Fig. 2 shows a typical stress distribution of the un-reinforced composite panel with a 44 mm diameter cutout under an in-plane shear load of 20 N/mm (equivalent to an applied constant shear stress of 10 MPa). The plot shows the stress map in the local fibre direction of a ply with fibre orientation in the -45° direction. The maximum stress at the cutout edge is about 91 MPa.

The FE results are compared with an isotropic (aluminium) panel of the same size and same cutout in order to find out if the stress concentration in the composite panel will vary with the cutout size in the same order of magnitude as the isotropic plate. Table 2 gives the maximum stress of the isotropic panel and the through-thickness averaged in-plane stress at the same point at the cutout edge of the composite panel as indicated by the insert sketch of Fig. 2. Firstly, the maximum stresses in both panels increase with the increasing cutout size as expected. Although the cross-ply laminate $(\pm 45)_{4S}$ has a slightly severer stress concentration under the same applied load, the magnitude of stress concentration is about the same to that of the isotropic plate. Secondly, for the intermediate cutout (64 mm), the maximum stress in both panels does not increase significantly with the cutout size. However, for the largest cutout (160 mm) the maximum stress is almost doubled the value of the smallest cutout (44 mm). Finally, for illustration purpose, the maximum stress at the same reference point in a single ply (-45°) in the fibre direction is also given in Table 2. Since the scope of this paper is to study the effect of cutout and reinforcement on stress concentration and buckling stability, material failure analysis based on stress and material strength is not included in this paper. There are many published research addressing the issue of failure prediction at cutouts.

At the early design stage, it may be desirable or practical to estimate stress concentration by an engineering approach based on the ESDU datasheet [18] as reviewed in the Section 2 of this paper. Since this method was developed using an infinitely large laminate, the stress solution is independent of the cutout size. To evaluate this method against different cutout sizes, it was compared with the FE results in terms of the average in-plane stress in the x axis. For the 44 mm diameter cutout size, the maximum tensile stress in the x -axis was 29.1 MPa. An alternative FE model based on the equivalent elastic modulus of the whole laminate, i.e. $E_x = E_y = 13.88$ GPa (Table 1) yielded an average stress of 26.2 MPa. The ESDU approach gives stress value of 31 MPa. Comparison of the three stress results shows a fairly good agreement between the FE models and the rather simple engineering method [18] for this relatively small cutout size. For the intermediate cutout diameter, e.g. $d=64$ mm, the difference in the maximum stress between the FE models and the ESDU method is slightly larger. Since the latter is an approximate method and independent of the cutout size, a poorer agreement between the FE and ESDU data was found when the cutout diameter was increased to 160 mm. Therefore, the engineering approach is only applicable for the small and intermediate cutouts, i.e. cutout ratio $d/a < 0.2$.

3.3 Effect of cutout on buckling stability

As the cutout size and consequently the stress concentration increase, the reduction in stability of a constant stress-loaded panel is expected in terms of the buckling load factor (BLF = critical buckling load / applied load). For the metallic and composite panels under applied shear load of 20 N/mm with simply-supported and clamped conditions, the buckling loads up to the first five modes have been obtained by FE analysis and given in Table 3. Since the BLF in all the modes vary in the same trend with the cutout size, the effect of cutout size on buckling stability can be demonstrated by plotting the first mode BLF in Fig. 3. It is noted that the composite panel with the largest cutout diameter (160 mm) will buckle under the applied constant shear stress. In this figure, BLF = 1.8 for a

panel without cutout obtained from ESDU 80023 [21] has been included for comparison purpose. Since the ESDU data is limited to a specially orthotropic plate, i.e. $[0, 90]_{ns}$, the result for this particular example is only an approximate.

4. Reinforced Cutouts

From above analysis it is noted that the metallic plate with different cutout sizes and without reinforcement performs better than its composite counterpart in terms of the buckling load factor. In some plies of the composite panel the stress concentration at the cutout is much higher than that in metal panel, but composites can normally carry much higher stresses. An interactive failure criterion, e.g. Tsai-Hill criterion, can be used to determine the strength of the composite panel, but this is beyond the scope of this paper.

The purpose of this paper is to explore whether or not with suitable reinforcement composite panels can perform at least as good as their metallic counterparts and thus be employed in shear-loaded components when large cutouts are involved, e.g. ribs or spar webs with lightening holes. Four different cutout reinforcements have been designed to investigate their effectiveness in improving stress concentration and buckling stability. These reinforcements are: a flanged cutout, a bonded composite ring, a flanged cutout and a composite ring, and double rings on each side as illustrated in Fig. 4.

Finite element analyses have been performed for the above configurations made of composite and aluminium materials. To simplify the result presentation, only the 44 mm diameter cutout results are presented for discussing stress concentration effect, but the BLF values are presented for the whole range of cutout in order to show the cutout size effect.

Type 1 – Flange Reinforcement. The effect of different flange angle ϕ and height h on the maximum stress at the cutout edge in the fibre direction and the stability has been studied. Table 4 shows a larger reduction in stress was achieved for the composite plate (up to 16.5%) comparing with the metallic plate (2.4%). This flange reinforcement will add weight to structure that is equivalent to 1/3 of the cutout material weight. The results also show improvements in buckling stability for all three cutout sizes and the same level of effectiveness for both materials. It is noted however that the out-of-plane unsymmetrical geometry may cause a shear-bending coupling and reduce the effectiveness of reinforcement in stability.

Type 2 – Single ring reinforcement. In this type of reinforcement, a composite ring of the same material and layup as the laminated panel with various width and thickness was bonded on one side of the panel around the cutout. As shown in Table 5, this reinforcement resulted in a stress reduction by up to 18.4% for the composite panel and 13.7% for the metallic plate. The same level of improvement in panel's stability as that of the type 1 reinforcement has been achieved. However it adds a weight penalty due to the reinforcement ring being equivalent to 2.6 times of the cutout material weight. Like the type 1 reinforcement the unsymmetrical geometry in z-axis may reduce the effectiveness of reinforcement in terms of stability.

Type 3 – Flange and ring reinforcement. A composite ring of width $w_r=20$ mm and $t_r=2$ mm was bonded on the opposite side to the flanged cutout of type 1 as shown in Fig. 4. This reinforcement resulted in a large reduction of maximum stress by up to 30.3% for the composite panel and 16.6% for the metallic panel as shown in Table 6. This double sided reinforcement resulted in a significantly larger improvement in stability for the panel with the largest cutout. However, only a little more improvement was achievable for the smaller cutout comparing with the type 1 and 2 reinforcements. The weight penalty was equivalent to 2.9 times of the cutout material weight.

Type 4 – Double ring reinforcement. Reinforcement rings were bonded on both sides of the shear panel around the cutout. The reinforcement ring material and size varied to enable parametric study. When a pair of composite rings (same as the type 2) was employed, more significant reduction in the stress at the cutout edge and increase in BLF have been achieved comparing with previous reinforcement types. Results are presented in Table 7. When the composite rings were replaced by a pair of metallic rings of width $w_r = 15$ mm and thickness $t_r = 2$ mm, more stress reduction was achieved depending upon the alloy material. A comparison of the maximum stress with all reinforcement types and reinforcement materials studied in this paper is presented in Fig. 5. In the figure the stress values presented are the calculated maximum stress in a ply at the vicinity of the cutout in the local fibre direction under the applied shear force of 20 N/mm (equivalent to shear stress of 10 MPa). The first column in Fig. 5 shows the maximum stress in an unreinforced panel as the control case (Fig. 2 shows the stress distribution in this case). It is noted that the double ring reinforcement resulted in the most significant reduction in stress concentration and the best improvement in buckling stability. Regarding the ring materials, it is noted that the higher the material modulus the more load the ring will carry; hence less stress concentration in the shear panel. Therefore, despite being heavier, metallic rings perform noticeably better than cross-ply composite rings.

5. Experiment and Comparison with FEA

5.1 Test samples

To validate the finite element results, selective samples from the above design ranges were experimentally tested. Laminated plates with cutout of 44 mm diameter and reinforcement type 2 and 4 were selected with details listed in Table 8. The samples were made of unidirectional pre-preg of 914C-HTA with stacking sequence of $(45/-45)_{4S}$ and the cutouts were fabricated after curing. The metallic and composite rings were then manufactured and bonded to the composite panel using epoxy adhesive Araldite 420 A/B.

For test sample 1, four strain gauge rosettes of gauge factor 2.11 were mounted close to the cutout edge at 45° and 135° from the x -axis on both sides of the plate as illustrated in Fig. 6. For sample 2, rosette gauges were located as shown in Fig. 7. Since it was difficult to place the gauges near the cutout edge or on the narrow ring on the back side where the reinforcement ring was bonded, gauge D was placed away from the cutout edge to be comparable with gauge C position. For sample 3 where composite rings were bonded on both sides, all rosette gauges were located outside the ring with two additional small gauges (No. 13 and 14) of size 6 mm and gauge factor 1.88 glued on to the ring at an angle of 45° as illustrated in Fig. 8a. For test sample 4, however, all rosette gauges were attached on the steel ring of 15 mm wide and near the cutout edge as shown in Fig. 8b.

5.2 Test rig design

The test machine (RDP Avery) has the load capability of 600 kN. A shear load rig made of steel was designed and manufactured as shown in Fig. 9, which was then mounted to the machine at the bottom of the jig. The test plate was bolted to the shear load rig along one vertical edge and loaded downward along the opposite edge as shown in Fig. 9. To prevent the plate from buckling before the load reached 6.4 kN, which is equivalent to a shear intensity of 20 N/mm or shear stress of 10 MPa, the top and bottom edges of the plate were reinforced by steel strips bolted on both sides.

5.3 Test results and data analysis

From the measured strains, stresses at the measurement locations can be calculated based on following equations [18]:

$$\sigma_x = \frac{E_x}{(1-\nu_{xy}\nu_{yx})} \varepsilon_x + \frac{\nu_{yx}E_x}{(1-\nu_{xy}\nu_{yx})} \varepsilon_y \quad (1)$$

$$\sigma_y = \frac{\nu_{xy}E_y}{(1-\nu_{xy}\nu_{yx})} \varepsilon_x + \frac{E_y}{(1-\nu_{xy}\nu_{yx})} \varepsilon_y \quad (2)$$

Sample 1 – un-reinforced cutout. For the plate without reinforcement, strains versus loads measured at point B (see Fig. 6) are presented in Fig. 10. The strain values corresponding to applied load of 6.4 kN, which gives 10 MPa shear stress along the panel edge, are listed in Table 9. According to equation (1), these strain values were converted to stress of $\sigma_x = 76$ MPa. The strains were actually measured a few millimetres away from the cutout edge at point B as illustrated in Fig. 6. This was for the purpose of comparison of the stress with that of reinforced cutouts where the gauges were bonded just outside the ring (see Figs. 6 and 7, gauge points B and D). The FE result taken for comparison is in the same position. As shown in Fig. 2, the stress in that region near the hole edge varies from 72 to 84 MPa giving the average of 78 MPa, which agrees very well with the stress value 76 MPa that is calculated from the measured strains.

Sample 2 –single composite ring reinforcement. Strains measured at point D as illustrated in Fig. 7 are presented in Fig. 11. The strains corresponding to 6.4 kN load and the converted stress are listed in Table 9. Comparing with the FE result of $\sigma_x = 40.1$ MPa taken at the same location, a good agreement has been reached.

Sample 3 – double composite rings. Strains measured at point C (Fig. 8a) are presented in Fig. 12. The strains corresponding to applied load of 6.4 kN and the resulting stress are listed in Table 9. Again, the results show a very good agreement between the test data and FE results.

Sample 4 – double steel rings. For the plate reinforced by double steel rings, strains measured at point B on the ring (Fig. 8b) are presented in Fig. 13. The strains and the resulting stress are also listed in Table 9. The FE stress result (Fig. 14) shows that the stress on the ring varies and the value in the middle of the ring is about 23.7 MPa, which is very close to the measured average strain in this area.

Finally, the critical buckling load from the experimental and FE results under simply supported condition are summarised in Table 10 for comparison. Good agreement has been achieved.

5.4 Comparison and discussions

The experimental results have confirmed the accuracy of the FE results of stress and BLF. Therefore, FEA can be used as a tool to investigate a wider range of reinforcement designs in terms of geometry and materials.

Regarding the local stress at cutout edge, all four types of reinforcement have resulted in large reduction of stress concentration in the composite panels. Among them, the type 4 reinforcement is the most effective one with the maximum reduction of local stress by up to 53%. For the metallic shear panel, reinforcement type 3 and type 4 have resulted in large stress reduction by up to 17% and 50%, respectively. For reinforcement type 1 and type 2, however, although considerable stress reduction is achieved on the reinforced side of the plate, slightly higher stress has occurred on the un-reinforced side.

In terms of buckling stability of the panels, reinforcement type 1 is much more effective and practical for metallic panels with various cutout sizes than composite ones. Reinforcement type 2 and type 3 are also more effective for the metallic panels than the

composite ones with small (44 mm) and medium (64 mm) sized cutouts. However as the cutout size increases to 160 mm, these types of reinforcement for the composite plate would reach almost the same level of stability improvement as for the metallic plate. The type 4 reinforcement using two composite rings was only slightly less effective but very competitive comparing with the metallic panels having all cutout sizes. The use of metallic rings for cutout reinforcement (type 4) is most effective, as well as being practical providing an easier and cheaper manufacturing option. It will also make the mounting of a structural part such as a pipe going through the cutout much easier.

Considering both stress reduction and stability improvement, the effectiveness of the type 4 reinforcement is about double that of type 1. However this achievement is at the cost of more weight penalty. Nevertheless, by replacing a large aluminium shear panel with a composite one will result in a larger weight saving and offset the relatively small weight penalty due to the metallic reinforcement rings.

6. Conclusions

All four types of reinforcement are more effective for the composite shear panel than the metallic panel in terms of reducing the cutout induced stress concentrations.

Reinforcement type 1 (flanged edge) is a practical solution and most effective for metallic shear panels in improving the buckling stability when weight saving is a concern. However it may not be feasible for the composite shear panels due to the manufacturing difficulty and relatively small improvement in buckling stability.

For the small and medium sized cutouts, reinforcement type 2 (single ring) and type 3 (combined ring and flange) are more effective for the metallic panels than for the composite ones. For the large cutout ($d/a = 0.5$), however, performance of reinforced composite panels is competitive to that of the metallic ones in terms of stress concentration and buckling stability; the former also offers more weight savings.

Reinforcement type 4 (double rings) is the best option for composite shear panels. A pair of high modulus metallic rings provides the most effective reinforcement in both reduced stress concentration and increased buckling stability.

Acknowledgement

The author is most grateful to KC Pang and LC Zhou for their valuable contribution towards the experimental testing and FE analysis reported in this paper.

References

1. Turvey GJ, Marshall IH. *Buckling and postbuckling of composite plates*. Chapman & Hall, 1995. ISBN 0 412 59120 0. (Chapter 8 by Nemesh MP)
2. Nemeth MP. Buckling and postbuckling behaviour of laminated composite plates with a cutout, *NASA Technical Paper 3587*, July 1996.
3. Martine J. Buckling and postbuckling of laminated composite square plates with reinforced central holes, *PhD Dissertation*, Case Western Reserve University, 1972.
4. Knauss JF, Starnes, JH Jr., Henneke EG. The compressive failure of graphite/epoxy plates with circular holes, *VPI-E-78-5*, Virginia Polytechnic Inst. & State University, Feb. 1978.
5. Marshall IH, Little W, EI Tay MM. The stability of composite panels with holes. *Proceedings of Reinforced Plastic Congress*, Brighton, UK, 1984, pp.139-142.

6. Marshall IH, Little W, EI Tay MM. The stability of composite panels with holes. *Mechanical Characterization of Load Bearing Fibre Composite Laminates*, Cardon AH and Verchery G Eds., 1985, pp.235-242.
7. Nemeth MP. A buckling analysis for rectangular orthotropic plates with centrally located cutouts. *NASA TM-86263*, 1984.
8. Chang CN, Chiang, FK. Stability analysis of a thick plate with interior cutout, *AIAA Journal*, 1999; 28:1285-1291.
9. Turvey, GJ, Sadeghipour, K. Shear buckling of anisotropic fibre-reinforced rectangular plates with central circular cutouts. *Computer Aided Design in Composite Material Technology: Proceedings of the International Conference*, Carlos A. Brebbia, Blain WR and De Wilde WP eds., April 1988, pp.459-473.
10. Owen VL, Klang EC. Shear buckling of specially orthotropic plates with centrally located cutouts. *In: Eighth DOD/NASA/FAA Conference on Fibrous Composites in Structural Design*, Part 2, Sept. 1990, pp. 695-706.
11. Rouse, M. Effect of cutouts or low-speed impact damage on the postbuckling behaviour of composite plates loaded in shear. *31st AIAA/ASME/ASCE/AHS/ASC Structures, Structural Dynamics and Materials Conference*, Long Beach, CA, Apr. 1990, pp. 877-891.
12. Jones KM, Klang EC. Buckling analysis of fully anisotropic plates containing cut-outs and elastically restrained edges. *Proc. 33rd AIAA/ASME/ASCE/AHS/ASC Structures, Structural Dynamics and Materials Conference*, April 1992, pp.190-200.
13. Britt VO. Shear and compression buckling analysis for anisotropic panels with centrally located elliptical cutouts. *Proc. 34th AIAA/ASME/ASCE/AHS/ASC Structures, Structural Dynamics and Materials Conference*, La Jolla, CA, Apr. 1993, pp. 2240-2249.
14. Kim YH, Noor AK. Buckling and postbuckling of composite panels with cutouts subjected to combined loads. *Finite Elements in Analysis and Design*, 1996, 22:163-185.
15. Eiblmeier J, Loughlan, J. The buckling response of carbon fibre composite panels with reinforced cut-outs, *Composite Structures*, 1995; 32: 97-113.
16. Pandey, R, Thakur, S, Ramanath, KS, Rao, KP. Stress concentration and stability studies in composite ribs with flanged cutouts. *In: 2001 World MSC Aerospace Conference*, Toulouse, France, September 24-26, 2001.
17. Greszczuk, LB. Stress concentrations and failure criteria for orthotropic and anisotropic plates with circular openings. *ASTM STP 497*, 1971. pp. 363-381.
18. ESDU 85001. *Elastic Stress and Strain Distributions around Circular Holes in Infinite Plates of Orthotropic Material (Applicable to Fibre Reinforced Composites)*. Published by ESDU International, 1985.
19. ESDU 86003. *Choice of reinforcement for a circular hole in a fibre reinforced laminate plate*. Published by ESDU International, 1986.
20. ESDU 75034. Initial buckling stress, maximum direct stress and shear strain of square plates in shear with central circular holes. Published by ESDU International, 1975.
21. ESDU 80023. Buckling of rectangular specially orthotropic plates. Published by ESDU International, 1980.

Tables

Table 1. Material properties for the panels studied in this paper.

AL 7075-4045	E = 71.02 (GPa)		G = 26.89 GPa	$\nu = 0.33$
Layer (ply) elastic constants	E ₁₁	E ₂₂	G ₁₂	ν_{12}
	113.97 (GPa)	8.13 (GPa)	3.89 (GPa)	0.315
Panel (laminates) equivalent constants	E _x = E _y	G _{xy}	ν_{xy}	ρ
	13.88 (GPa)	29.45 (GPa)	0.783	1560 (Kg/m ³)

Table 2. Stress concentration in the panels under applied shear stress 10 MPa

Cutout ratio (d/a)	0.137	0.2	0.5
Maximum stress in the metallic panel (MPa)	42.2	45.1	83.2
Average maximum stress in the composite panel (MPa)	49.2	53.2	106.3
Maximum ply stress in the composite panel (MPa)	91.1	95.3	200.5

Table 3. Buckling load factors (BLF) of the panels with unreinforced cutouts.

Cutout ratio (d/a)	Buckling Load Factor (BLF)				
	mode 1	mode 2	mode 3	mode 4	mode 5
	Metallic (simply-supported)				
0.137	2.022	-2.022	3.009	-3.009	6.302
0.2	1.766	-1.766	2.914	-2.914	4.683
0.5	0.753	-0.753	1.019	-1.019	1.490
	Composite (simply-supported)				
0.137	1.321	-1.698	1.774	-2.290	3.543
0.2	1.164	-1.493	1.724	-2.223	2.633
0.5	0.534	-0.638	0.642	-0.778	0.839
	Composite (clamped)				
0.137	1.787	-2.277	2.459	-3.140	4.036
0.2	1.571	-1.991	2.320	2.891	-2.963
0.5	0.760	0.787	-0.898	-0.938	1.054

Table 4. Panels with type-1 (flanged) reinforcement: Maximum stress (MPa) and BLF.

Cutout	flange angle ϕ (deg)	0	32	32	45	45
ratio d/a	height h (mm)	0	5	10	5	10
0.137	stress of composite panels	91.1	79.2	82.5	77.5	76.1
0.137	stress of metallic panels	42.2	43.5	43.4	43.3	41.2
0.137	BLF	1.32	1.58	1.70	1.55	1.643
0.2	of composite panels	1.16	1.54	1.71	1.50	1.649
0.5	(simply-supported)	0.53	1.07	1.59	1.00	1.51
0.5	BLF of metallic panels	0.75	1.64	2.34	1.55	2.26
0.137	BLF	1.79	2.22	2.44	2.17	2.33
0.2	of composite panels	1.57	2.16	2.44	2.10	2.34
0.5	(clamped)	0.76	1.57	2.33	1.45	2.19

Table 5. Panels with type 2 reinforcement: Maximum stress (unit: MPa) and BLF.

Cutout	ring width w_r (mm)	0	10	10	20	30
ratio d/a	ring thickness t_r (mm)	0	2	4	2	2
0.137	stress of composite panels	91.1	85.3	79.3	77.9	74.3
0.137	stress of metallic panels	42.2	44.5	41.6	39.8	36.4
0.137	BLF	1.32	1.69	1.81	1.89	1.97
0.2	of composite panels	1.16	1.66	1.93	1.93	2.16
0.5	(simply-supported)	0.53	1.04	1.72	1.34	1.64
0.5	BLF of metallic panels	0.75	1.59	2.63	2.09	2.52
0.137	BLF	1.79	2.39	2.63	2.73	2.91
0.2	of composite panels	1.57	2.36	2.84	2.80	3.27
0.5	(clamped)	0.76	1.53	2.50	1.96	2.39

Table 6. Panels with type 3 reinforcement: Maximum stress (unit: MPa) and BLF.

Cutout	flange angle β (deg)	0	32	32	45	45
ratio d/a	height h (mm)	0	5	10	5	10
0.137	stress of composite panels	91.1	73.9	64.9	69.1	63.5
	stress of metallic panels	42.2	38.9	36.2	38.6	35.2
0.137	BLF	1.32	1.74	1.46	1.68	1.57
0.2	of composite panels	1.16	1.80	1.57	1.76	1.67
0.5	(simply-supported)	0.53	1.60	2.70	1.69	2.58
0.5	BLF of metallic panels	0.75	2.38	3.37	2.58	3.71
0.137	BLF	1.79	2.49	2.07	2.35	2.20
0.2	of composite panels	1.57	2.60	2.33	2.52	2.43
0.5	(clamped)	0.76	2.35	4.19	2.43	3.69

Table 7. Panels with type 4 reinforcement: Maximum stress (unit: MPa) and BLF.

Cutout ratio d/a	ring width w_r (mm)	0	10	10	20	30
	ring thickness t_r (mm)	0	2	4	2	2
0.137	stress of composite panels	91.1	46.6	38.5	44.1	42.8
0.137	stress of metallic panels	42.2	26.4	20.4	23.6	21.1
0.137	BLF of composite panels (simply-supported)	1.32	1.79	1.82	1.86	1.95
0.2		1.16	1.88	1.94	2.02	2.16
0.5		0.53	1.54	2.88	2.25	3.07
0.5	BLF of metallic panels	0.75	2.25	4.23	3.37	4.63
0.137	BLF of composite panels (clamped)	1.79	2.59	2.59	2.70	2.88
0.2		1.57	2.76	2.84	3.02	3.33
0.5		0.76	2.24	4.19	3.28	4.44

Table 8. Test samples with different types of reinforcement.

Test sample No	Reinforcement Type	Ring width w_r (mm)	Ring thickness t_r (mm)
1	Unreinforced cutout	0	0
2	Type 2 (single composite ring)	10	2
3	Type 4 (two composite rings)	10	2
4	Type 4 (two steel rings)	10	2

Table 9. Comparison of maximum stress between experiment and FE results of the panels subjected to shear load 6.4 kN

Sample No	Measurement point	Measured $\varepsilon_x \times 10^{-3}$	Measured $\varepsilon_y \times 10^{-3}$	Converted stress σ_x (MPa)	FE σ_x (MPa)
1	B	1.8	0.4	76	78
2	D	1.1	0.2	45.1	40.1
3	C	0.7	0.02	25.7	25.3
4	B	0.085	0.04	21.3	23.7

Table 10. Comparison of buckling load between experiment and FE results.

Test sample	1	2	3	4
Experiment (kN)	8.5	9.5	10.0	10.5
FE (kN)	8.4	10.8	11.5	11.8

Figures

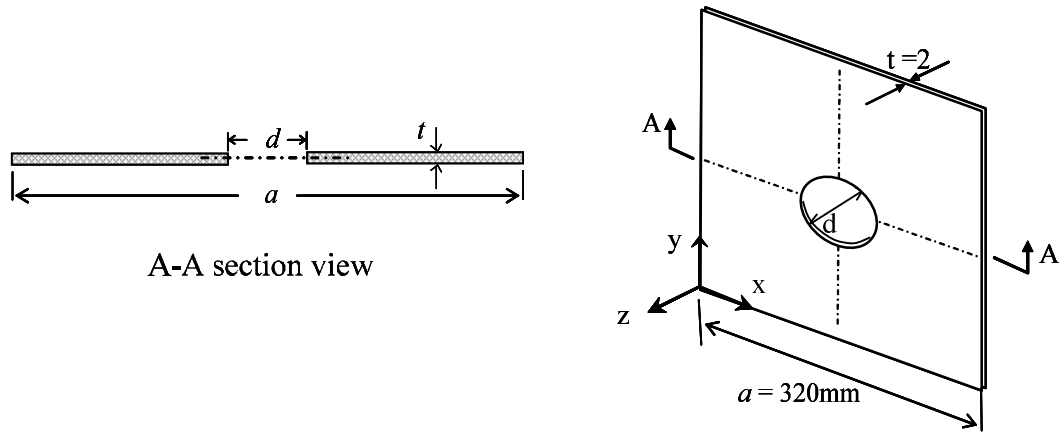


Figure 1. Composite panel with a central circular cutout ($d=44, 64, 160$ mm).

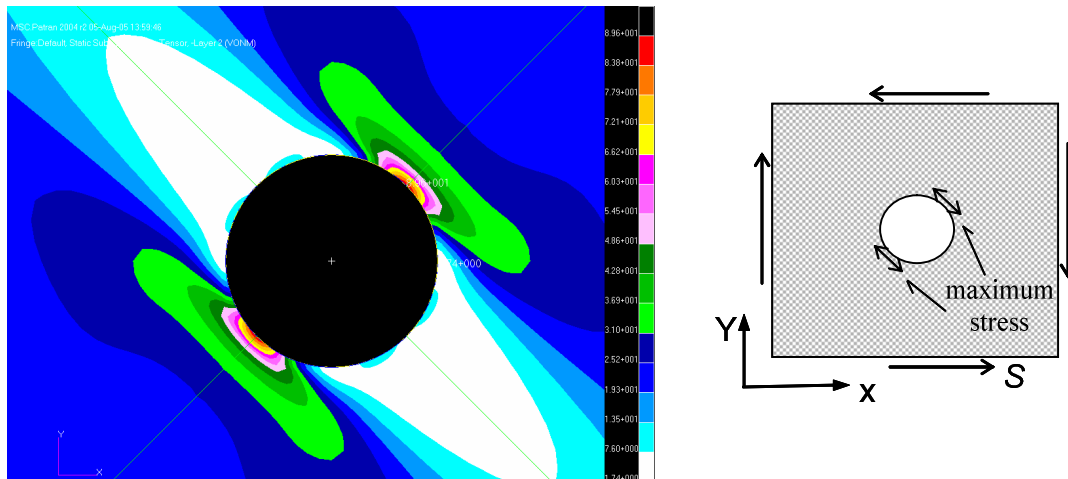


Figure 2. Stress distribution around un-reinforced cutout (Insert sketch shows the applied shear load $S=20$ N/mm and maximum stress location and direction).

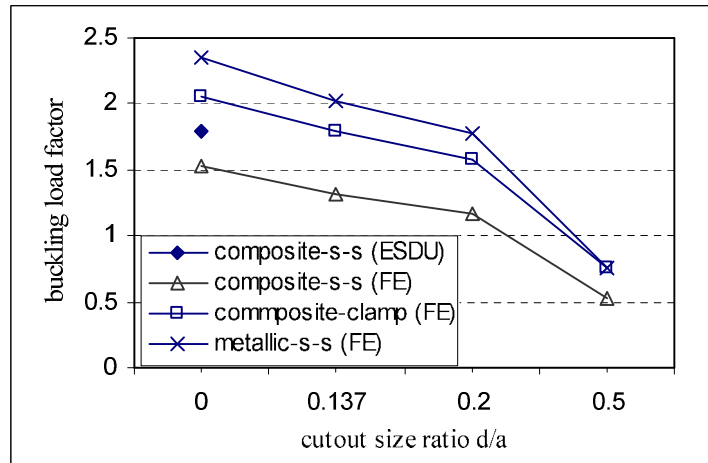


Figure 3. Variation of buckling load factor with cutout size for shear-loaded composite and metallic panels (s-s denotes simply-supported edges; clamp denotes fully clamped edges).

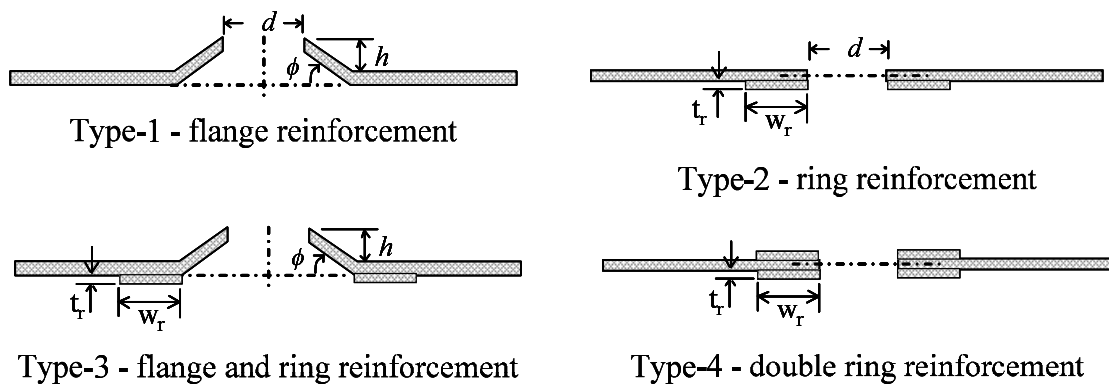


Figure 4. Four types of cutout reinforcement studied in this paper.

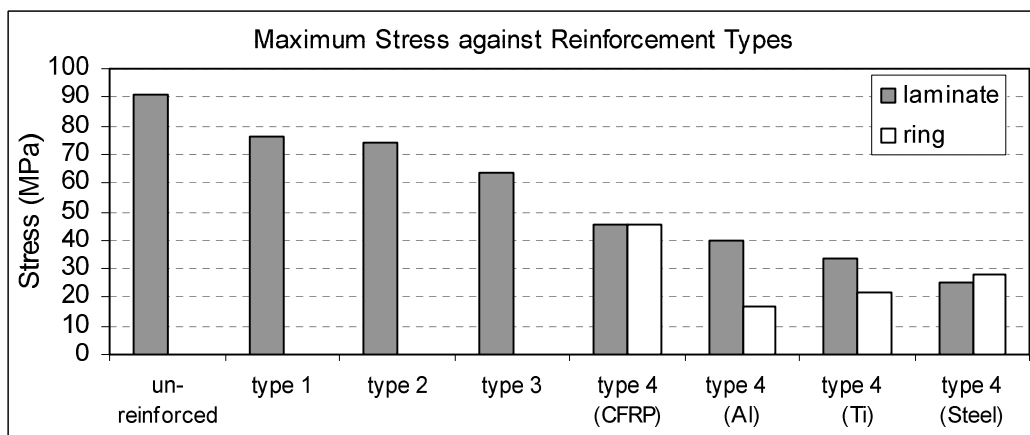


Figure 5. Comparison of maximum stress with different reinforcement types. Note: The stress values presented are the calculated maximum stress at the vicinity of the cutout in fibre direction under an applied constant shear stress of 10 MPa.

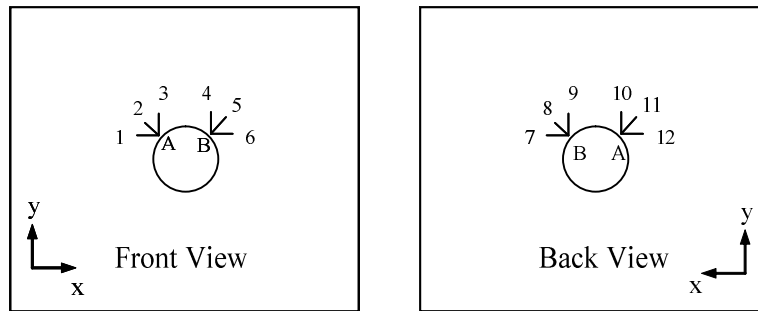


Figure 6. Strain gauge locations for test sample 1 without reinforcement

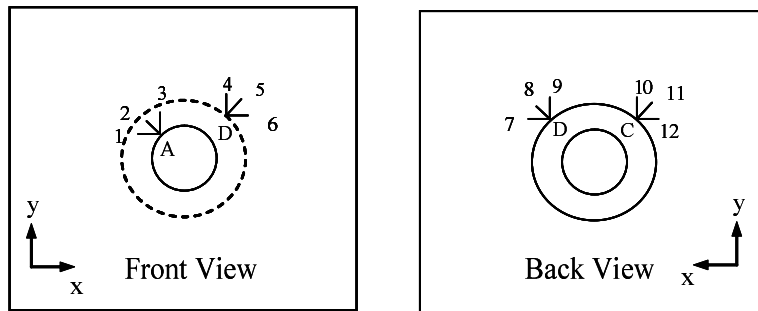


Figure 7. Strain gauge locations for test sample 2 with single ring reinforcement

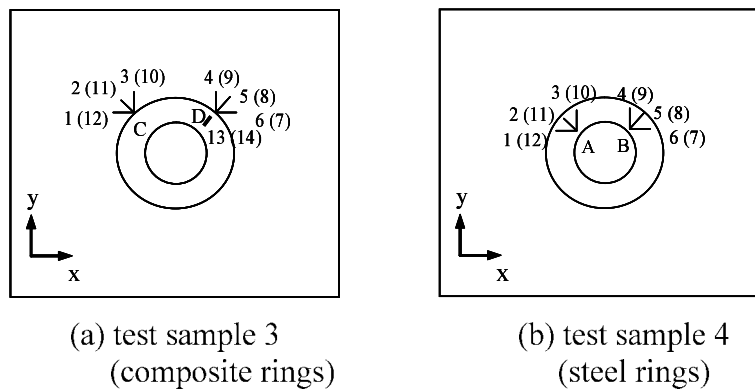


Figure 8. Strain gauge locations for test samples 3 and 4 with double rings (gauge numbers in brackets indicate those gauges on the back side).

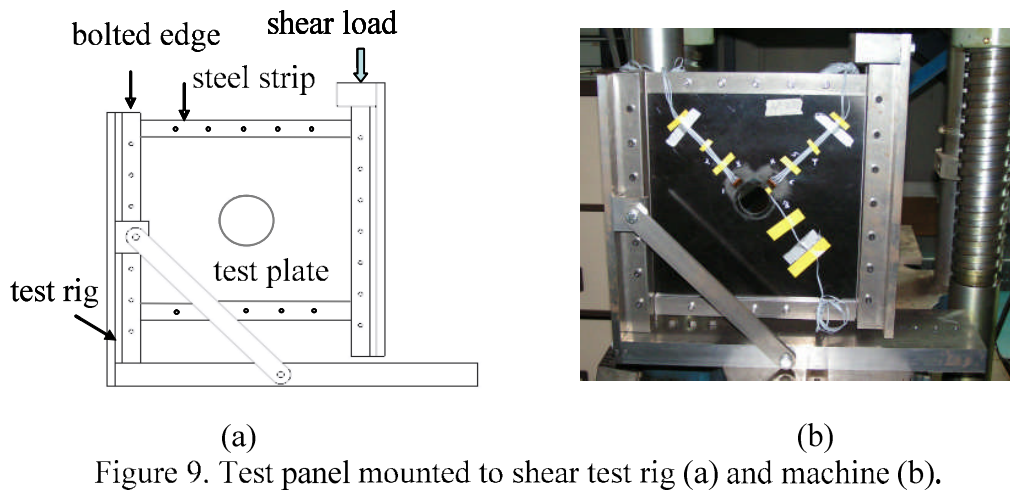


Figure 9. Test panel mounted to shear test rig (a) and machine (b).

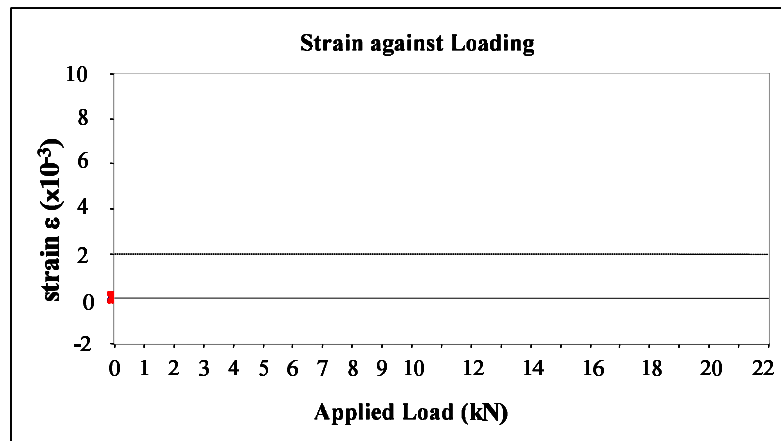


Figure 10. Measured strain against applied shear load in test sample 1

Figure 11. Measured strain against applied shear load in test sample 2